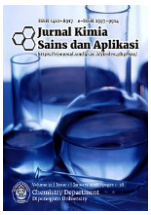
ISSN: 1410-8917
Jurnal Kimia Sains & Aplikasi
e-ISSN: 2597-9914

Jurnal Kimia Sains dan Aplikasi 29 (9) (2026): 631-640

Jurnal Kimia Sains dan Aplikasi
Journal of Scientific and Applied Chemistry

Journal homepage: http://ejournal.undip.ac.id/index.php/ksa



Synthesis of 1-Hydroxy-6-methoxyxanthone and Comparison of Its α-Glucosidase Inhibitory and Antibacterial Activities with Hydroxyxanthone Derivatives

Nela Fatmasari [1,*], Clara Shabrina Parameswary [1], Ken Hastu Mulamawarni [1], Faris Hermawan [2], Minarti [2], Yoga Mulya Ramadhan [3], Fadhil Ardiyan Syahputra [3], Minandre Wiratama [3], Reinhard Sharon Lase [4], Muhammad Badrul Huda [5]

[1] Chemistry Education, Sultan Ageng Tirtayasa University, Serang, Banten 42117, Indonesia
[2] Research Center for Pharmaceutical Ingredients and Traditional Medicine, National Research and Innovation Agency (BRIN), Tangerang Selatan, Banten 15314, Indonesia
[3] Department of Chemistry, Faculty of Military Mathematics and Natural Sciences, Universitas Pertahanan Republik Indonesia, Bogor, Indonesia
[4] Department of Chemistry, Universitas Negeri Semarang, Kampus Sekaran, Gunungpati, Semarang 50229, Indonesia
[5] Chemistry Department, Faculty of Sciences and Mathematics, Diponegoro University, Jl. Prof. Soedarto, SH., Tembalang, Semarang, Indonesia

* Corresponding author: nela.fatmasari@untirta.ac.id

https://doi.org/10.14710/jksa.29.9.631-640

Article Info

Article history:

Received: 21st August 2026
Revised: 16th September 2026
Accepted: 09th October 2026
Online: 30th October 2026

Keywords:
Antibacterial activity; Molecular docking; Synthesis; 1-Hydroxy-6-methoxyxanthone; α- Glucosidase inhibition

Abstract

Xanthone derivatives have attracted considerable interest owing to their broad spectrum of biological activities, making them promising scaffolds for the development of multifunctional therapeutic agents. In this study, 1-hydroxy-6-methoxyxanthone (**MX1**) was synthesized via cyclodehydration using Eaton's reagent, affording the target compound in 18.50% yield, and structurally characterized by FTIR, LC–MS, and NMR spectroscopy. **MX1** was obtained as a yellow solid in 18.50% yield, with a melting point of 145–147°C. The α- glucosidase inhibitory and antibacterial activities of **MX1** were evaluated in comparison with those of previously reported hydroxyxanthone derivatives (**HX1–HX3**), while molecular docking was performed to investigate their binding interactions with α-glucosidase. Among the evaluated compounds, **MX1** exhibited the most potent α-glucosidase inhibitory activity with an IC_{50} value of 203.23 µg/mL, followed by **HX2** (223.53 µg/mL), whereas **HX1** and **HX3** showed weaker inhibition, with IC_{50} values of 463.74 and 482.86 µg/mL, respectively. Molecular docking demonstrated that all compounds occupied a common binding pocket and formed favorable interactions with key active-site residues through hydrogen bonding, $\pi-\pi$, and π–anion interactions, supporting the proposed structure–activity relationships. In contrast, **MX1** exhibited limited antibacterial activity, with MIC values of 500 µg/mL against *Pseudomonas aeruginosa* and *Bacillus subtilis* and >1000 µg/mL against *Escherichia coli* and *Staphylococcus aureus*. Collectively, these findings indicate that replacement of the C-6 hydroxyl group with a methoxy group enhances α-glucosidase inhibitory activity while reducing antibacterial activity, underscoring the pivotal role of C-6 substitution in modulating the biological activities of xanthone derivatives.

1. Introduction

Diabetes mellitus (DM) is a prevalent metabolic disorder characterized by chronic hyperglycemia, which can lead to severe complications, including cardiovascular diseases, nephropathy, neuropathy, and retinopathy [1]. Among the therapeutic strategies for controlling postprandial hyperglycemia, inhibition of intestinal α-glucosidase has proven effective by delaying

the hydrolysis of dietary carbohydrates into absorbable monosaccharides [2]. Clinically available α-glucosidase inhibitors, such as acarbose and miglitol, effectively reduce postprandial glucose and insulin responses [3]. However, their clinical use is frequently associated with gastrointestinal adverse effects, including flatulence, abdominal pain, abdominal discomfort, and diarrhea, highlighting the need for safer and more effective α-glucosidase inhibitors [4].

In addition to diabetes, antimicrobial resistance (AMR) has emerged as another major global health challenge, compromising the effectiveness of existing antibiotics and increasing the morbidity and mortality, as well as the economic burden, associated with bacterial infections [5] Moreover, the rapid emergence of multidrug-resistant bacteria has substantially limited available treatment options, emphasizing the urgent need to develop novel antibacterial agents with improved efficacy and distinct mechanisms of action [6]. Collectively, these challenges have stimulated growing interest in developing multifunctional compounds with both antidiabetic and antibacterial activities, a promising strategy in medicinal chemistry.

Xanthones are an important class of oxygen-containing heterocyclic compounds that have attracted considerable attention in medicinal chemistry for their diverse pharmacological properties, including antioxidant, anti-inflammatory, antimicrobial, antidiabetic, and anticancer activities [7, 8, 9, 10, 11]. Among the numerous xanthone derivatives, hydroxyxanthones have attracted particular attention because hydroxyl substitution substantially influences their biological activities and provides valuable insights into the structure–activity relationships of xanthone-based compounds [12]. The importance of hydroxyl substitution has been further demonstrated by studies on α-glucosidase inhibition. Liu *et al.* [13] synthesized a series of mono-, di-, tri-, and tetrahydroxyxanthones and demonstrated that hydroxyl substitution markedly enhanced α-glucosidase inhibition compared with the parent xanthone. Notably, polyhydroxylated xanthones exhibited the highest inhibitory activities, indicating that both the number and position of hydroxyl substituents play important roles in modulating enzyme inhibition.

Hydroxyxanthone derivatives have also shown promising antibacterial activity, which is strongly influenced by the position and number of hydroxyl substituents on the xanthone scaffold. Yuanita *et al.* [14] reported the antibacterial activity and molecular docking of hydroxyxanthone derivatives against several bacterial pathogens. In our previous study, 1,5-dihydroxyxanthone (**HX1**), 1,6-dihydroxyxanthone (**HX2**), and 1,7-dihydroxyxanthone (**HX3**) exhibited distinct antibacterial profiles against Gram-positive and Gram-negative bacteria. **HX1** and **HX3** showed MIC values of 15.62 µg/mL against *S. aureus* and *B. subtilis*, whereas **HX2** showed MIC values of 31.25 µg/mL against both bacteria. All three compounds showed an MIC of 15.62 µg/mL against *P. aeruginosa*, but none inhibited *E. coli* at concentrations up to 1000 µg/mL [15]. However, the α-glucosidase inhibitory activities of **HX1**–**HX3** were not investigated in our previous study, leaving the relationship between their hydroxyl substitution patterns and α-glucosidase inhibition unexplored. Although 1-hydroxy-6-methoxyxanthone (**MX1**) has been reported previously, its biological evaluation varies across the available studies. Wang *et al.* [16] synthesized **MX1** by methylation of a hydroxyxanthone precursor and evaluated its α-glucosidase inhibitory activity. Heilman *et al.* [17] reported **MX1**, a xanthone isolated from a plant source; however, they did not report experimental antibacterial activity for **MX1**.

In the present study, **MX1** was synthesized via a one-pot cyclodehydration reaction, offering an alternative synthetic approach. This provides an opportunity to comparatively investigate the biological profile of **MX1** alongside hydroxyxanthones with different hydroxyl substitution patterns. In particular, comparison of **MX1** with **HX2** is of interest because these compounds share the same xanthone framework and differ only in the substituent at the C-6 position. Such a comparison may clarify how hydroxyl-to-methoxy substitution at C-6 is associated with differences in α-glucosidase inhibitory and antibacterial activities under the same experimental conditions, rather than implying a causal structure–activity relationship.

Therefore, this study aimed to synthesize and characterize **MX1** and comparatively evaluate its α-glucosidase inhibitory and antibacterial activities alongside those of the previously reported hydroxyxanthones **HX1**–**HX3**. Molecular docking was further performed to investigate their interactions with α-glucosidase and provide structural insights into the observed inhibitory activities.

2. Experimental

Commercially available chemicals and solvents were obtained from Sigma-Aldrich and Merck and used directly without further purification unless otherwise stated. The progress of all reactions was monitored by analytical thin-layer chromatography (TLC) on silica gel 60 F_{254} plates (Merck), with detection under UV irradiation at 254 and 366 nm. ^{1}H and ^{13}C NMR spectra were recorded on a Bruker Ascend 700 MHz NMR spectrometer at operating frequencies of 700 and 176 MHz, respectively, using CD_3OD as the deuterated solvent. Chemical shifts were reported in ppm (δ) relative to the residual solvent signal. Mass spectra were acquired using an LC-MS/MS Xevo G2-XS QTOF mass spectrometer (Waters MS Technologies) equipped with an electrospray ionization (ESI) source, while FTIR spectra were recorded on a Shimadzu Prestige-21 spectrometer.

2.1. Synthesis of 1-hydroxy-6-methoxyxanthone (MX1)

A mixture of 2,6-dihydroxybenzoic acid (2.5 mmol) and 3-methoxyphenol (2.5 mmol) was prepared in commercial Eaton's reagent (phosphorus pentoxide (P_2O_5) in methanesulfonic acid (MSA), Sigma-Aldrich) (2.5 mL) in a three-neck round-bottom flask. The reaction mixture was maintained at 80°C with continuous stirring for 3 h under a reflux condenser. The progress of

the reaction was monitored by TLC using a hexane/ethyl acetate (2:1, v/v) solvent system.

After completion of the reaction, cold distilled water was added to the mixture, followed by stirring for an additional 30 min to promote product precipitation. The precipitate was collected by filtration, washed with distilled water, and dried in an oven for 24 h. The resulting crude product was purified by column chromatography using hexane/ethyl acetate (2:1, v/v) as the eluent. The purified 1-hydroxy-6-methoxyxanthone (**MX1**) was obtained as a yellow solid (18.50% yield) with a melting point of 145–147°C. The identity and purity of **MX1** were supported by FTIR, ^{1}H NMR, ^{13}C NMR, and LC–MS characterization.

Yellow solid; yield: 18.50%. FTIR (cm^{-1}) 3718, 2947, 1602, 1441, 1278, 1123, 765. ^{1}H NMR ^{1}H-NMR (700 MHz, CD_3OD) δ 8.17 (d, *J* = 8.7 Hz, 1H, H-8), 7.64 (t, *J* = 8.3 Hz, 1H, H-3), 7.08–7.03 (m, 2H, H-5 and H-7), 6.99 (dd, *J* = 8.4, 1.0 Hz, 1H, H-4), 6.78 (dd, *J* = 8.2, 1.0 Hz, 1H, H-2), 3.98 (s, 3H, OCH_3). ^{13}C-NMR (176 MHz, CD_3OD) δ 181.33 (C-9), 166.33 (C-6), 161.61 (C-1), 158.41 (C-4b), 156.46 (C-4a), 136.25 (C-3), 126.88 (C-8), 113.88 (C-8a), 113.55 (C-7), 109.96 (C-2), 108.20 (C-8b), 106.61 (C-4), 99.87 (C-5), 55.29 (C-10, OCH_3). LC-MS/MS (ESI-QTOF) m/z 243.0650 $[M+H]^+$ (calcd for $C_{14}H_{11}O_4^+$, 243.0652), consistent with the proposed molecular formula of **MX1**. The chemical structures of HX1–HX3 and MX1 are shown in Figure 1.

2.2. α-Glucosidase Inhibitory Assay

The α-glucosidase inhibitory activities of the synthesized hydroxyxanthone derivatives (**HX1–HX3**) and **MX1** were evaluated using *p*-nitrophenyl-α-D-glucopyranoside (*p*NPG) as the substrate. The assay was performed according to Wibawa *et al.* [18], with slight modifications. Stock solutions of the test compounds were prepared by dissolving 2 mg of each compound in 250 µL of dimethyl sulfoxide (DMSO) to obtain a concentration of 8 mg/mL. The stock solutions were subsequently diluted with DMSO to prepare test solutions at final concentrations ranging from 12.5 to 800 µg/mL.

An aliquot (5 µL) of each sample solution was transferred into a 96-well microplate containing 45 µL of phosphate buffer (0.1 M, pH 6.8), followed by the addition of 25 µL of 5 mM *p*NPG solution. The mixture was pre-incubated at 37°C for 5 min, after which 25 µL of α-glucosidase from *Saccharomyces cerevisiae* (1.5 U/mL) was added to initiate the enzymatic reaction. The reaction mixture was further incubated at 37°C for 15 min and subsequently terminated by adding 100 µL of 0.2 M Na_2CO_3 solution. The absorbance was measured at 405 nm using a microplate reader (Epoch, BioTek Instruments, Winooski, VT, USA).

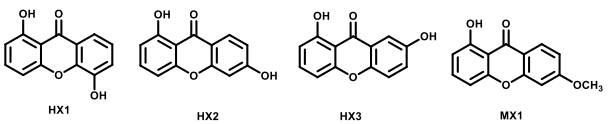


Figure 1. Chemical structures of **HX1–HX3** and **MX1**

For each test concentration, an enzyme-free sample blank was prepared using the corresponding sample solution without α-glucosidase. Quercetin was used as the positive control at concentrations ranging from 0.782 to 50 µg/mL. A DMSO vehicle control was included at an equivalent concentration to that present in the assay wells. All experiments were performed in triplicate. The percentage inhibition of α-glucosidase activity was calculated according to Equation (1).

$$Inhibition\ (\%) = \frac{[(A_{b1}-A_{b0})-(A_{s1}-A_{s0})]}{(A_{b1}-A_{b0})} \times 100\% \qquad (1)$$

where A_{b1} is the absorbance of the control reaction containing enzyme but without inhibitor, A_{b0} is the absorbance of the control blank without enzyme, A_{s1} is the absorbance of the sample in the presence of enzyme, and A_{s0} is the absorbance of the sample blank without enzyme.

2.3. Antibacterial Activity

The antibacterial activity of **MX1** was evaluated against a panel of reference bacterial strains obtained from the Research Center for Pharmaceutical Ingredients and Traditional Medicine, National Research and Innovation Agency (BRIN), Indonesia. The tested strains included *Pseudomonas aeruginosa* (*P. aeruginosa*) ATCC 9027, *Escherichia coli* (*E. coli*) ATCC 8739, *Bacillus subtilis* (*B. subtilis*) ATCC 6633, and *Staphylococcus aureus* (*S. aureus*) ATCC 25923. The minimum inhibitory concentration (MIC) and minimum bactericidal concentration (MBC) of **MX1** were determined using the broth microdilution method [19].

MX1 was dissolved in methanol and serially diluted twofold to obtain concentrations ranging from 7.81 to 1000 µg mL^{-1}. The prepared solutions were mixed with Mueller–Hinton broth (MHB) and dispensed into sterile 96-well microplates to obtain a total volume of 100 µL per well. Bacterial cultures were adjusted to a 0.5 McFarland standard using 0.85% NaCl before being inoculated into the wells. The microplates were incubated at 37°C for 24 h with shaking at 150 rpm. Tetracycline was used as the positive control, and methanol as the negative/vehicle control. A sterility control containing MHB without bacterial inoculum was also included. The MIC was defined as the lowest concentration of **MX1** showing no visible bacterial growth. For MBC determination, aliquots from the MIC well and higher concentrations showing no visible growth were transferred onto Mueller–Hinton agar (MHA) and incubated at 37°C for 24 h. The MBC was defined as the lowest concentration at which no bacterial colonies were observed. All experiments were performed in triplicate.

2.4. Molecular Docking

The molecular structures of **HX1–HX3** and **MX1** were constructed using Avogadro and subsequently optimized at the DFT/B3LYP/6-31G level using the ORCA program. The optimized structures were exported in PDB format for molecular docking studies [20, 21]. The crystal structure of *Saccharomyces cerevisiae* α-glucosidase (PDB ID: 3A4A) was retrieved from the Protein Data Bank and prepared using UCSF Chimera by removing crystallographic water molecules, co-crystallized ligands, and unnecessary

heteroatoms, followed by the addition of hydrogen atoms and assignment of partial atomic charges [22].

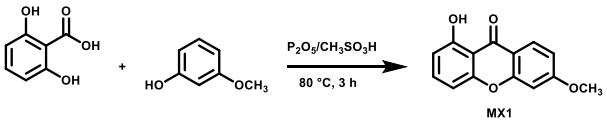
The docking protocol was validated by re-docking the co-crystallized ligand into the enzyme active site using AutoDockTools 1.5.6 and AutoDock4 [23]. The alpha-D-glucopyranose (GLC) ligand was used exclusively for docking validation and was not included as a compound in the in vitro α-glucosidase inhibition assay. The accuracy of the docking protocol was evaluated by calculating the root-mean-square deviation (RMSD) between the crystallographic and re-docked GLC poses, with an RMSD value of ≤2.0 Å considered acceptable.

A 30 × 30 × 30 grid box with a spacing of 0.375 Å was centered on the active site. Docking simulations were performed using the Lamarckian Genetic Algorithm (LGA), with 50 independent runs per ligand. The validated protocol was subsequently used to dock **HX1**–**HX3** and **MX1**. The binding pose with the lowest predicted binding energy was selected for subsequent protein–ligand interaction analysis using BIOVIA Discovery Studio Visualizer [24]. Quercetin, used as the positive control in the in vitro assay, was also subjected to molecular docking to compare with the synthesized xanthone derivatives.

3. Results and Discussion

3.1. Synthesis of 1-hydroxy-6-methoxyxanthone (MX1)

MX1 was successfully synthesized via a one-pot cyclodehydration reaction between 2-hydroxy-6-methoxybenzoic acid and 3-methoxyphenol using Eaton's reagent as both the solvent and dehydrating agent (Scheme 1). The reaction proceeded smoothly under reflux at 80°C for 3 h, affording **MX1** as a yellow crystalline solid after purification. The isolated yield of **MX1** was 18.50%. The relatively low yield may be attributed to the substrate-dependent selectivity of Eaton's reagent-mediated xanthone synthesis. Bosson [25] demonstrated that the electronic properties and substitution patterns of both salicylic acid and phenol substrates strongly influence the reaction outcome, with electronically unfavorable substrates potentially undergoing competing reactions and forming benzophenone or regioisomeric products. In contrast, highly electron-rich phenols such as phloroglucinol favor xanthone formation. Thus, the use of 2-hydroxy-6-methoxybenzoic acid and 3-methoxyphenol may contribute to the modest isolated yield of **MX1**.



Scheme 1. Synthetic route of **MX1**

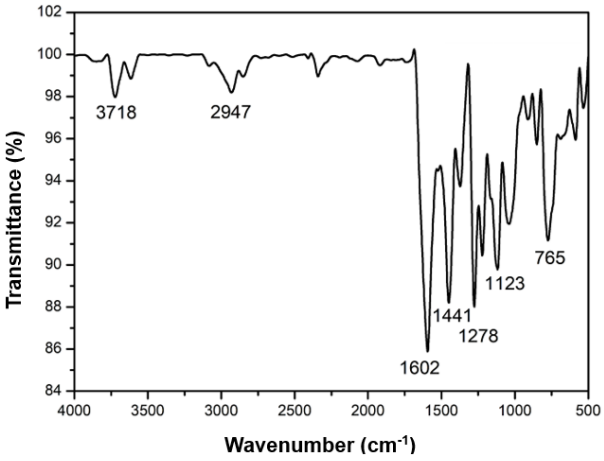


Figure 2. FTIR spectra for compound **MX1**

The structure of **MX1** was confirmed by FTIR, LC–MS, and NMR spectroscopy. The FTIR spectrum exhibited a sharp absorption band at 3718 cm^{-1}, assigned to phenolic O–H stretching, and a strong band at 1602 cm^{-1}, attributed to the conjugated carbonyl (C=O) stretching vibration of the xanthone framework. This assignment is consistent with previous reports on xanthone and hydroxyxanthone derivatives, in which the characteristic xanthone carbonyl absorption has been reported in the ~1600–1660 cm^{-1} region, with hydroxyl substitution capable of shifting the carbonyl stretching frequency to lower wavenumbers [14]. Additional absorption bands at 1278 and 1123 cm^{-1} were assigned to C–O stretching vibrations of the methoxy and aryl ether groups, respectively (Figure 2).

The LC–MS spectrum displayed a protonated molecular ion peak at *m*/z 243.1 $[M + H]^+$, consistent with the molecular formula of MX1 and confirming its molecular weight. Additionally, the ^1H NMR spectrum of **MX1** was consistent with the proposed molecular structure. A singlet integrating for three protons appeared at δ 3.98 ppm, corresponding to the methoxy group ($-OCH_3$) (Figure 3). The relatively upfield chemical shift is characteristic of methyl protons attached to an oxygen atom and is consistent with values reported for structurally related methoxyxanthone derivatives.

The aromatic region displayed six proton resonances in accordance with the substitution pattern of the xanthone nucleus. The signals at δ 6.78 (dd, *J* = 8.2, 1.0 Hz) and δ 6.99 (dd, *J* = 8.4, 1.0 Hz) were assigned to H-2 and H-4, respectively, each exhibiting ortho and meta coupling with neighboring aromatic protons. The overlapping signals observed at δ 7.08–7.03 ppm were attributed to H-5 and H-7. Meanwhile, H-3 resonated as a triplet at δ 7.64 ppm (*J* = 8.3 Hz), indicating coupling with two adjacent aromatic protons. The most downfield signal at δ 8.17 ppm appeared as a doublet (*J* = 8.7 Hz) and was assigned to H-8.

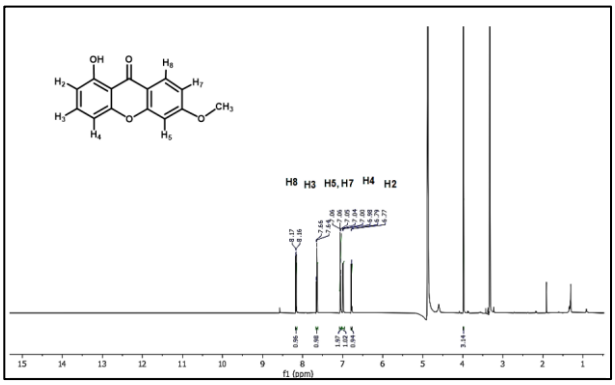


Figure 3. H-NMR spectra for compound **MX1**

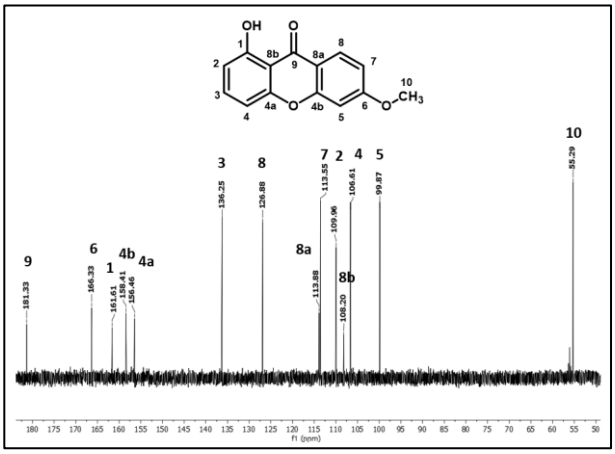


Figure 4. C-NMR spectra for compound **MX1**

The ^{13}C NMR spectrum of **MX1** exhibited 14 carbon resonances, consistent with the proposed molecular structure (Figure 4). The signal at δ 55 ppm was assigned to the methoxy carbon (C-10), characteristic of a methyl carbon bonded to an oxygen atom. The resonance at δ 181 ppm corresponded to the carbonyl carbon (C-9) of the xanthone skeleton, confirming the presence of the conjugated ketone functionality. Two downfield signals at δ 166 and 161 ppm were attributed to the oxygenated aromatic carbons C-6 and C-1, respectively, bearing the methoxy and hydroxyl substituents. In addition, the resonances at δ 158 and 156 ppm were assigned to the bridgehead carbons C-4b and C-4a, respectively, which are bonded to the central ether oxygen of the xanthone framework. The remaining resonances in the δ 100–137 ppm region were assigned to the aromatic carbons of the xanthone skeleton. Overall, the combined FTIR, LC–MS, ^{1}H NMR, and ^{13}C NMR spectroscopic data were in good agreement with the proposed structure, confirming the successful synthesis of **MX1**.

3.2. α-Glucosidase Inhibitory Activity

The α-glucosidase inhibitory activities of the previously synthesized **HX1**–**HX3** and the newly synthesized **MX1** were evaluated using the *p*NPG assay, and the results are presented in Table 1. The *p*NPG assay is based on the enzymatic hydrolysis of *p*NPG by α-glucosidase, which releases *p*-nitrophenol (*p*NP) and glucose. Under alkaline conditions, *p*NP is converted to its yellow *p*-nitrophenolate form, allowing the enzymatic reaction to be monitored spectrophotometrically at approximately 405 nm. The tested xanthone derivatives do not directly react with *p*NPG but inhibit α-glucosidase, thereby reducing pNPG hydrolysis and the subsequent formation of *p*NP. Consequently, stronger enzyme inhibition results in lower absorbance, and the inhibitory activity is expressed as the IC_{50} value [26].

All compounds exhibited measurable inhibitory activity against α-glucosidase, although their inhibitory potencies remained substantially lower than that of quercetin, the positive control. Among the hydroxyxanthone derivatives, **HX2** showed the lowest IC_{50} point estimate, with an IC_{50} of 223.53 ± 45.72 µg/mL, whereas **HX1** and **HX3** showed IC_{50} values of 463.74 ± 176.40 and 482.87 ± 105.98 µg/mL, respectively. **MX1** showed a slightly lower IC_{50} point estimate than **HX2**, at 203.24 ± 9.34 µg/mL under the assay conditions used. However, its inhibitory potency was substantially lower than that of quercetin, which exhibited an IC_{50} value of 6.74 µg/mL. Thus, **MX1** exhibited measurable but limited α-glucosidase inhibitory potency relative to quercetin, and further optimization and biological evaluation are required to assess its potential as a lead compound.

The differences in inhibitory activity suggest that the α-glucosidase inhibitory potential of xanthone derivatives is strongly influenced by the substitution pattern on the xanthone scaffold. Although **HX1**–**HX3** possess the same number of hydroxyl groups, their inhibitory activities varied considerably, indicating that the position of the hydroxyl substituents plays an important role in enzyme inhibition. Furthermore, **MX1** showed a slightly lower IC_{50} point estimate than **HX2** under the assay conditions used, suggesting that the methoxy-substituted xanthone exhibited a modest difference in α-glucosidase inhibitory activity compared with the corresponding hydroxy analog.

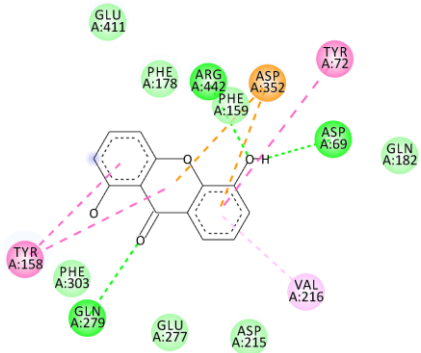
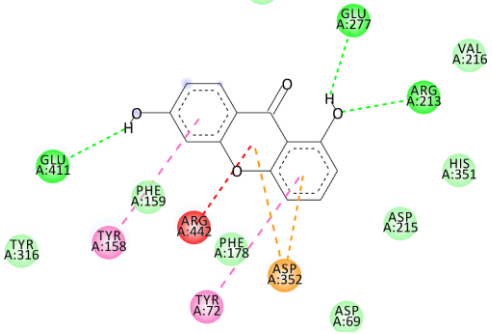
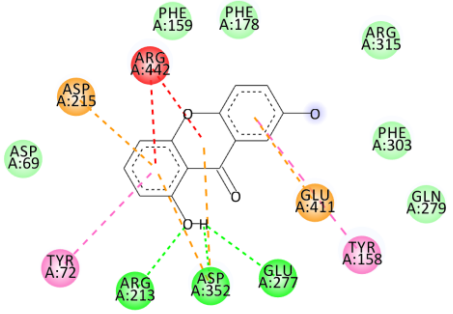
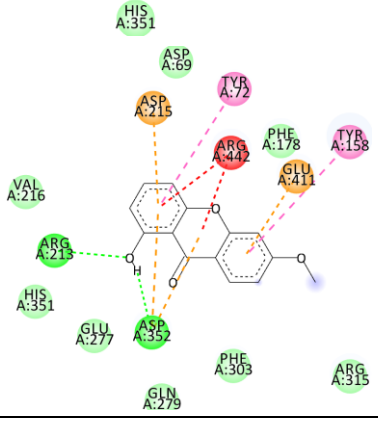
3.3. Molecular Docking Analysis

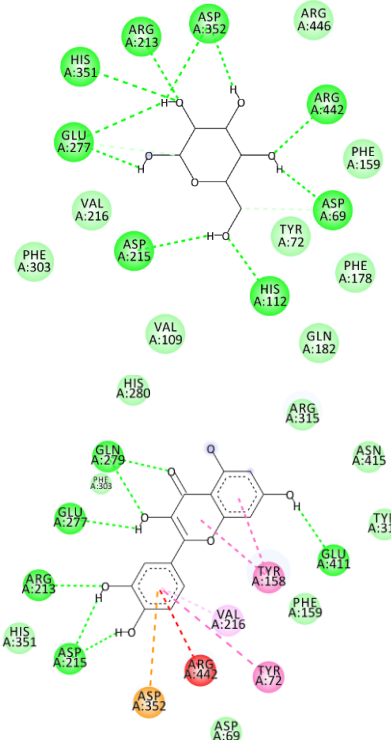
To elucidate the molecular basis of the observed α-glucosidase inhibitory activities, molecular docking simulations were performed using the α-glucosidase active site. The calculated binding energies and ligand–protein interactions are presented in Table 2. All xanthone derivatives exhibited favorable binding affinities, with binding energies ranging from -5.69 to -6.43 kcal/mol, although these values were slightly higher than those of the native ligand α-D-glucopyranose (-6.99 kcal/mol) and quercetin (-7.01 kcal/mol). Among the synthesized compounds, **HX1** showed the lowest binding energy (-6.43 kcal/mol), followed by **HX2** (-6.37 kcal/mol), **MX1** (-6.26 kcal/mol), and **HX3** (-5.69 kcal/mol).

Table 1. α-Glucosidase inhibitory activity of compounds **HX1**–**HX3** and **MX1**

Compound	IC_{50} (µg/mL)
HX1	463.74 ± 176.40
HX2	223.53 ± 45.72
HX3	482.87 ± 105.98
MX1	203.24 ± 9.34
Quercetin	6.74 ± 0.36

Table 2. Binding energies and 2D interaction diagrams of compounds **HX1**–**HX3** and **MX1**

Compound	Binding energy (kcal/mol)	2D-interactions
HX1	-6.43	
HX2	-6.37	
HX3	-5.69	
MX1	-6.26	

Compound	Binding energy (kcal/mol)	2D-interactions
α-D-glucopyranose	-6.99	
Quercetin	-7.01	

Overall, the docking results showed a qualitative relationship with the experimental α-glucosidase inhibitory activities. Quercetin exhibited the most favorable binding energy (-7.01 kcal/mol) and the strongest inhibition (IC_{50} = 6.74 µg/mL), while **HX3** showed the least favorable binding energy (-5.69 kcal/mol) and the weakest inhibition among the xanthone derivatives (IC_{50} = 482.86 µg/mL). **HX2** and **MX1** also exhibited comparable binding energies (-6.37 and -6.26 kcal/mol) and similar inhibitory activities (IC_{50} = 223.53 and 203.23 µg/mL, respectively). **HX1** was the main deviation, exhibiting a relatively favorable binding energy (-6.43 kcal/mol) but weaker inhibitory activity (IC_{50} = 463.74 µg/mL). This deviation indicates that docking energy alone may not fully account for the experimental inhibitory activity, although the overall binding-energy and IC_{50} trends provide qualitative support for the observed structure–activity relationship [27, 28, 29].

Analysis of the binding modes revealed that all xanthone derivatives occupied a similar binding pocket and interacted with several common amino acid residues through conventional hydrogen bonds, π–anion, π–π T-shaped, and hydrophobic interactions (Table 2). The major interacting residues included Arg213, Arg442, Asp352, Tyr72, Tyr158, Glu277, and Glu411, indicating that the xanthone scaffold was well accommodated within the active site of α-glucosidase. Among the hydroxyxanthones, **HX2** and **MX1**, which exhibited the lowest IC_{50} values, showed distinct predicted interaction patterns with the α-glucosidase active site compared with **HX1** and **HX3**. **HX2** formed three conventional hydrogen bonds with Glu411, Glu277, and Arg213, together with a π-anion interaction with Asp352 and a π-cation interaction with Arg442, as well as π–π T-shaped interactions with Tyr72 and Tyr158. In comparison, **MX1** formed conventional hydrogen bonds with Arg213 and Asp352, together with π-anion interactions involving Asp215 and Glu411, a π-cation interaction with Arg442, and π–π T-shaped interactions with Tyr72 and Tyr158. These findings indicate distinct predicted interaction patterns among the xanthone derivatives.

Although **MX1** showed a slightly lower IC_{50} point estimate than **HX2** under the assay conditions used, the docking results alone do not establish that methoxy substitution enhances α-glucosidase inhibitory activity. Notably, **HX2** and **MX1** differ only in the substituent at the C-6 position. In **HX2**, the C-6 hydroxyl group formed a conventional hydrogen bond with Glu411, whereas this interaction was not observed for **MX1** after replacement of the hydroxyl group with a methoxy group. This substitution removes the hydrogen-bond donor capability of the C-6 substituent and consequently alters the interaction pattern within the binding site. Nevertheless, **MX1** retained interactions with other key residues, including Arg213, Asp352, Arg442, Asp215, Tyr72, and Tyr158.

Table 3. Antibacterial activity of compounds **HX1**–**HX3** and **MX1**

Compound	MIC (µg/mL)				Reference
	E. coli	*P. aeruginosa*	*S. aureus*	*B. subtilis*	
HX1	>1000	15.62	15.62	15.62	[14]
HX2	>1000	15.62	31.25	31.25	[14]
HX3	>1000	15.62	15.62	15.62	[14]
MX1	>1000	500	>1000	500	This work
Compound	MBC (µg/mL)				Reference
	E. coli	*P. aeruginosa*	*S. aureus*	*B. subtilis*	
HX1	>1000	15.62	15.62	31.25	[14]
HX2	>1000	31.25	>62.5	>62.5	[14]
HX3	>1000	31.25	>31.25	31.25	[14]
MX1	>1000	>1000	>1000	500	This work

3.4. Antibacterial Activity

The antibacterial activities of the previously reported **HX1**–**HX3** and the newly synthesized **MX1** were evaluated against two Gram-negative bacteria (*E. coli* and *P. aeruginosa*) and two Gram-positive bacteria (*S. aureus* and *B. subtilis*). The MIC and MBC values are summarized in Table 3. Consistent with the previous study, **HX1**–**HX3** exhibited antibacterial activity against *P. aeruginosa*, *S. aureus*, and *B. subtilis*, with MIC values ranging from 15.62 to 31.25 µg/mL, whereas no inhibition was observed against *E. coli* at the highest tested concentration (MIC >1000 µg/mL). In contrast, the newly synthesized **MX1** was inactive against the tested bacterial strains, exhibiting MIC values of 500 µg/mL against *P. aeruginosa* and *B. subtilis*, and no inhibitory activity against *E. coli* and *S. aureus* at the highest concentration tested (MIC >1000 µg/mL). A similar trend was observed for the MBC values, where **HX1**–**HX3** exhibited bactericidal activity at relatively low concentrations, whereas **MX1** showed bactericidal activity only against *B. subtilis* at a relatively high concentration (MBC = 500 µg/mL).

HX2 and **MX1** differ only in the substituent at the C-6 position, where the hydroxyl group in **HX2** is replaced by a methoxy group in **MX1**. The antibacterial activity data for **HX1**–**HX3** were previously reported in our earlier study [14], whereas the data for **MX1** are reported for the first time in the present study. The compounds were evaluated under the same assay conditions, allowing direct comparison of their antibacterial activities. Under these comparable assay conditions, **MX1** showed lower antibacterial activity than **HX2**, suggesting that C-6 methylation may be associated with reduced antibacterial activity. Despite this subtle structural modification, **MX1** was inactive against the tested bacterial strains at the concentrations evaluated, whereas **HX2** exhibited substantially greater antibacterial activity, highlighting the contribution of the C-6 hydroxyl group to the antibacterial activity of xanthone derivatives. The presence of a free hydroxyl group at the C-6 position may facilitate hydrogen-bond formation with bacterial molecular targets or promote stronger interactions with bacterial cell components, whereas methylation of this functional group reduces its hydrogen-bond donor capability, thereby diminishing these interactions.

In contrast, the same structural modification exerted the opposite effect on α-glucosidase inhibition, with **MX1** exhibiting greater inhibitory activity than **HX2**. This observation highlights the distinct role of the C-6 substituent in modulating the biological profile of xanthone derivatives, where methylation was associated with reduced antibacterial activity but enhanced α-glucosidase inhibition. Collectively, these findings demonstrate that substitution at the C-6 position is a key structural determinant governing the biological activities of xanthone derivatives and that the structural requirements for antibacterial and α-glucosidase inhibitory activities are fundamentally different.

4. Conclusion

In this study, 1-hydroxy-6-methoxyxanthone (**MX1**) was successfully synthesized through cyclodehydration using Eaton's reagent and structurally confirmed by FTIR, LC–MS, and NMR spectroscopy. Biological evaluation demonstrated that **MX1** exhibited the strongest α-glucosidase inhibitory activity among the xanthone derivatives evaluated, although its potency remained substantially lower than that of quercetin. In contrast, **MX1** was inactive against the tested bacterial strains at the concentrations evaluated. Molecular docking revealed that all compounds interacted with key residues within the α-glucosidase active site, providing structural insights into the observed activity. Comparison between **MX1** and **HX2**, which differ only in the substituent at the C-6 position, demonstrated that replacement of the hydroxyl group with a methoxy group enhanced α-glucosidase inhibitory activity but abolished antibacterial activity under the tested conditions. These findings highlight the C-6 substituent as an important structural determinant of the biological profile of xanthone derivatives and provide a useful structure–activity relationship framework for further optimization of xanthone derivatives targeting α-glucosidase.

Acknowledgment

This work was supported by internal funding from Universitas Sultan Ageng Tirtayasa.

References

[1] D. Tomic, J. E. Shaw, D. J. Magliano, The burden and risks of emerging complications of diabetes mellitus, *Nature Reviews Endocrinology*, 18, 9, (2022), 525-539 https://doi.org/10.1038/s41574-022-00690-7

[2] U. Hossain, A. K. Das, S. Ghosh, P. C. Sil, An overview on the role of bioactive α-glucosidase inhibitors in ameliorating diabetic complications, *Food and Chemical Toxicology*, 145, (2020), 111738 https://doi.org/10.1016/j.fct.2020.111738

[3] M. Alssema, C. Ruijgrok, E. E. Blaak, L. Egli, P. Dussort, S. Vinoy, J. M. Dekker, M. Denise Robertson, Effects of alpha-glucosidase-inhibiting drugs on acute postprandial glucose and insulin responses: a systematic review and meta-analysis, *Nutrition & Diabetes*, 11, (2021), 11 https://doi.org/10.1038/s41387-021-00152-5

[4] S. R. Dehkordi, N. Pahlavani, M. Nikbaf-Shandiz, R. Bagheri, N. Rasaei, M. Darzi, S. Rastgoo, H. Bahari, F. Shiraseb, O. Asbaghi, A systematic review, meta-analysis, dose-response, and meta-regression of the effects of acarbose intake on glycemic markers in adults, *Journal of Diabetes & Metabolic Disorders*, 23, (2024), 135-172 https://doi.org/10.1007/s40200-023-01336-9

[5] C. J. L. Murray, K. S. Ikuta, F. Sharara, L. Swetschinski, G. Robles Aguilar, A. Gray, C. Han, C. Bisignano, P. Rao, E. Wool, S. C. Johnson, A. J. Browne, M. G. Chipeta, F. Fell, S. Hackett, G. Haines-Woodhouse, B. H. Kashef Hamadani, E. A. P. Kumaran, B. McManigal, M. Naghavi, Global burden of bacterial antimicrobial resistance in 2019: a systematic analysis, *The Lancet*, 399, 10325, (2022), 629-655 https://doi.org/10.1016/S0140-6736(21)02724-0

[6] C. R. MacNair, S. T. Rutherford, M. W. Tan, Alternative therapeutic strategies to treat antibiotic-resistant pathogens, *Nature Reviews Microbiology*, 22, (2024), 262-275 https://doi.org/10.1038/s41579-023-00993-0

[7] M. U. Azmi, N. I. Ramadhan, H. Margasari, F. N. Sari, L. N. Fitriani, T. S. Tjahjandarie, M. Tanjung, R. D. Saputri, Xanthone Derivatives from the Twigs of *Garcinia hombroniana* L. and Their Antioxidant Activity, *Tropical Journal of Natural Product Research*, 10, 5, (2026), 9476-9481 https://doi.org/10.26538/tjnpr/v10i5.63

[8] Z. Feng, X. Lu, L. Gan, Q. Zhang, L. Lin, Xanthones, A Promising Anti-Inflammatory Scaffold: Structure, Activity, and Drug Likeness Analysis, *Molecules*, 25, 3, (2020), 598 https://doi.org/10.3390/molecules25030598

[9] H. Li, W. T. Kang, Y. Zheng, Y. He, R. Zhong, S. Fang, W. Wen, S. Liu, S. Lin, Development of xanthone derivatives as effective broad-spectrum antimicrobials: Disrupting cell wall and inhibiting DNA synthesis, *Science Advances*, 11, 10, (2025), https://doi.org/10.1126/sciadv.adt4723

[10] R. Saikia, K. Pathak, P. Pramanik, M. A. Islam, S. Karmakar, S. Gogoi, M. P. Pathak, D. Das, J. J. Sahariah, M. Z. Ahmad, A. Das, Exploring the therapeutic potential of xanthones in diabetes management: Current insights and future directions, *European Journal of Medicinal Chemistry Reports*, 12, (2024), 100189 https://doi.org/10.1016/j.ejmcr.2024.100189

[11] G. Zhou, K. Dong, X. Xu, R. Guo, G. Li, J. Wang, L. Zhou, S. Yuan, H. Lou, H. Li, H. Dong, X. Peng, Fungal dimeric xanthones as anticancer agents by novelly stimulating sodium-calcium exchanger 1, *European Journal of Medicinal Chemistry*, 290, (2025), 117543 https://doi.org/10.1016/j.ejmech.2025.117543

[12] M. M. M. Pinto, A. Palmeira, C. Fernandes, D. I. S. P. Resende, E. Sousa, H. Cidade, M. E. Tiritan, M. Correia-Da-silva, S. Cravo, From Natural Products to New Synthetic Small Molecules: A Journey through the World of Xanthones, *Molecules*, 26, 2, (2021), 431 https://doi.org/10.3390/molecules26020431

[13] Y. Liu, L. Zou, L. Ma, W. H. Chen, B. Wang, Z. Le Xu, Synthesis and pharmacological activities of xanthone derivatives as α-glucosidase inhibitors, *Bioorganic & Medicinal Chemistry*, 14, 16, (2006), 5683-5690 https://doi.org/10.1016/j.bmc.2006.04.014

[14] E. Yuanita, I. M. Sudarma, N. M. Sudewiningsih, J. Syahri, N. K. T. Dharmayani, Sudirman, M. Ulfa, I. Sumarlan, Antibacterial activity and molecular docking studies of series hydroxyxanthone, *The 8th International Conference of The Indonesian Chemical Society (ICICS) 2019*, Bogor, Indonesia, 2020 https://doi.org/10.1063/5.0001090

[15] E. Fachriyah, M. B. Huda, P. R. Sarjono, F. Hermawan, R. S. Lase, N. Wijayati, J. Jumina, Y. D. Kurniawan, M. E. Prastya, Synthesis, Antibacterial Activity, and *In Silico* Analysis of Hydroxyxanthone Derivatives Targeting Gram-Positive and Gram-Negative Bacteria, *Indonesian Journal of Chemistry*, 26, 3, (2026), 948-962 https://doi.org/10.22146/ijc.113042

[16] L. Wang, C. Ai, C. Jin, J. Mou, Y. Deng, Xanthones as potential α-glucosidase non-competition inhibitors: Synthesis, inhibitory activities, and in silico studies, *Chemical Biology & Drug Design*, 102, 3, (2023), 547-556 https://doi.org/10.1111/cbdd.14272

[17] D. N. A. A. Heilman, A. Y. C. Hui, V. J. Y. Mian, F. B. Ahmad, L. P. Cee, J. Stanslas, N. H. Zamakshshari, Unlocking the Antibacterial Potential of Xanthone from Calophyllum Species: Inhibition of Nucleic Acid Synthesis, *Chemistry Select*, 8, 46, (2023), e202302737 https://doi.org/10.1002/slct.202302737

[18] I. P. A. H. Wibawa, F. Xavier, H. Verlianni, M. Minarti, P. D. Lotulung, M. Hanafi, *Pinanga arinasae* Witono, an endangered plant native to Bali, potentially as an antidiabetic and antioxidant, *Natural Product Research*, (2026), 1-5 https://doi.org/10.1080/14786419.2026.2632384

[19] E. N. W. Hening, J. A. Priyanto, M. E. Prastya, R. I. Astuti, L. O. A. P. Hasidu, Jamilah, Soil bacteria from Muna Island, Southeast Sulawesi, Indonesia: Antibacterial and antibiofilm activities, and the presence of antibiotic-biosynthetic genes, *Journal of Applied Pharmaceutical Sciences*, 14, 6, (2024), 207-217 https://doi.org/10.7324/japs.2024.171508

[20] M. D. Hanwell, D. E. Curtis, D. C. Lonie, T. Vandermeersch, E. Zurek, G. R. Hutchison, Avogadro: an advanced semantic chemical editor, visualization, and analysis platform, *Journal of*

Cheminformatics, 4, (2012), 17 https://doi.org/10.1186/1758-2946-4-17

[21] F. Neese, F. Wennmohs, U. Becker, C. Riplinger, The ORCA quantum chemistry program package, *Journal of Chemical Physics*, 152, 22, (2020), 224108 https://doi.org/10.1063/5.0004608

[22] E. F. Pettersen, T. D. Goddard, C. C. Huang, G. S. Couch, D. M. Greenblatt, E. C. Meng, T. E. Ferrin, UCSF Chimera—A visualization system for exploratory research and analysis, *Journal of Computational Chemistry*, 25, 13, (2004), 1605-1612 https://doi.org/10.1002/jcc.20084

[23] G. M. Morris, H. Ruth, W. Lindstrom, M. F. Sanner, R. K. Belew, D. S. Goodsell, A. J. Olson, AutoDock4 and AutoDockTools4: Automated docking with selective receptor flexibility, *Journal of Computational Chemistry*, 30, 16, (2009), 2785-2791 https://doi.org/10.1002/jcc.21256

[24] Biovia Dassault Systèmes, *Discovery Studio Visualizer (21.1.0.20298)*, Dassault Systèmes, 2021,

[25] J. Bosson, Scope and limitations of the preparation of xanthones using Eaton's reagent, *Turkish Journal of Chemistry*, 47, 6, (2023), 1420-1428 https://doi.org/10.55730/1300-0527.3624

[26] G. Granados-Guzmán, R. Castro-Ríos, N. Waksman de Torres, R. Salazar-Aranda, Optimization and Validation of a Microscale In vitro Method to Assess α-Glucosidase Inhibition Activity, *Current Analytical Chemistry*, 14, 5, (2018), 458-464 https://doi.org/10.2174/1573411013666170911154755

[27] J. Li, A. Fu, L. Zhang, An Overview of Scoring Functions Used for Protein–Ligand Interactions in Molecular Docking, *Interdisciplinary Sciences: Computational Life Sciences*, 11, (2019), 320-328 https://doi.org/10.1007/s12539-019-00327-w

[28] G. L. Warren, C. W. Andrews, A. M. Capelli, B. Clarke, J. LaLonde, M. H. Lambert, M. Lindvall, N. Nevins, S. F. Semus, S. Senger, G. Tedesco, I. D. Wall, J. M. Woolven, C. E. Peishoff, M. S. Head, A Critical Assessment of Docking Programs and Scoring Functions, *Journal of Medicinal Chemistry*, 49, 20, (2006), 5912-5931 https://doi.org/10.1021/jm050362n

[29] S. Y. Huang, S. Z. Grinter, X. Zou, Scoring functions and their evaluation methods for protein–ligand docking: recent advances and future directions, *Physical Chemistry Chemical Physics*, 12, 40, (2010), 12899–12908 https://doi.org/10.1039/c0cp00151a